PERGAMON

Chemical Engineering Science 57 (2002) 3749–3753

Chemical Engineering Science

www.elsevier.com/locate/ces

Practical chaotic mixing

M. M. Alvarez-Hernández, T. Shinbrot, J. Zalc, F. J. Muzzio *

Department of Chemical and Biochemical Engineering, School of Engineering, Rutgers University, 98 Brett Road, Piscataway, NJ 08854, 0909, USA

Received 29 May 2001; accepted 17 May 2002

Abstract

We present experimental and computational analyses of three-dimensional chaotic laminar mixing in one of the most widely utilized mixing devices, the stirred tank. We find that 98% of the power expended in mechanical stirring produces no detectable mixing at all, and in fact convective mixing is generated solely by tiny perturbations to a dominant non-chaotic flow. By analyzing the role of these perturbations, dramatic improvements in performance are easily achieved: for example, minor judicious, changes in agitator design produce order of magnitude improvements in mixing effectiveness.

1. Introduction

Mixing is simultaneously one of the most ancient and one of the least advanced technological practices. The processes of stirring, kneading and blending practiced by Paleolithic cave painters, who mixed soot and ochre with juice and animal fat (Graziosi, 1960), are easily recognized throughout today's food, drug, chemical, and semiconductor industries. Mixers, which are typically designed ad hoc, are among the most expensive and inefficient equipment in production plants (Kalk & Langlykke, 1986), and the annual cost of inefficient industrial mixing has been estimated to be as much as $10 billion in the US alone (Harnby, Edwards, & Nienow, 1992). Effects of this inefficiency can be dramatic (Epstein, 1995): for example, a 1993 nuclear-chemical waste explosion in Tomsk 7, Russia has been attributed to inadequate mixing of volatile compounds (Nuclear safety, 1995).

Researchers from Mathematics (Majda & McLaughlin, 1993), Physics (Sommerer & Ott, 1993), Geology (Pierrehumbert, 1991), Engineering (Aref, 1984), Chemistry (Graham et al., 1994) and Biology (Epstein, 1995) have investigated mixing processes in chaotic flows, however the overwhelming body of literature has focused on highly idealized systems (Harnby, Edwards, & Nienow, 1992; Epstein, 1995; Majda & McLaughlin, 1993; Aref, 1984), leaving details of most realistic mixing processes to the practitioner. Mixing processes are best understood in turbulent flows, where ironically they are only understood in a statistical sense. By comparison, detailed analysis of the mechanisms of realistic mixing processes in deterministic laminar flows is nearly absent from the literature.

A case in point is the stirred tank (ST). Although the ST is arguably the most common industrial mixer—used for the processing of detergents, creams, drugs, foods, vaccines and bulk chemicals—neither the Eulerian velocity field nor the Lagrangian particle trajectories have been accurately characterized in the laminar regime until very recently (Harvey & Rogers, 1996; Ranade, 1997; Harvey, Wood, & Leng, 1997; Lamberto, Alvarez, & Muzzio, 2001; Tanguy, Thibault, Brito-de la Fuente, Espinosa-Solares & Tecante, 1998; de la Villéon et al., 1998). Consider a prototypical example: a tank stirred by three co-axial "Rushton" impellers, each with six equally spaced vertical vanes, shown in Fig. 1(a). This figure shows the transport of fluorescent dye initially injected at the center of a tank illuminated from the side with a laser sheet. Under the conditions of the experiment, a small aliquot of dye will ultimately spread to cover approximately 80% of the cross-sectional area of the tank. If the impellers are replaced by disks of the same outer diameter (Fig. 1(b)), as we will demonstrate, a very similar flow is generated, but essentially no convective mixing

* Corresponding author. Tel.: +1-732-445-3357; fax: +1-732-445-2421.
E-mail address: muzzio@sol.rutgers.edu (F. J. Muzzio).

0009-2509/02/$ - see front matter © 2002 Elsevier Science Ltd. All rights reserved.
PII: S0009-2509(02)00265-8

occurs: dye injected *anywhere* in the flow becomes trapped in toroidal recirculating regions.

Conventional approaches that have been applied to date to analyze mixing flows provide little help in understanding mixing here: in Fig. 1(c) we show approximately 2 million successive intersections of fluid trajectories with a vertical plane within the tank from computational fluid dynamic calculations (described shortly). On the left of this figure, we display intersections using Rushton impellers, and on the right those generated by rotating disks. These "surfaces of section" (Alligood, Sauer, & Yorke, 1996) look almost identical and cannot be easily used to analyze mixing or to distinguish between the two systems. Moreover, both experiments and simulations demonstrate that vector velocity fields for the two flows (not shown) are extremely similar and the flows consume essentially identical amounts of energy, [1] yet as we have mentioned, the impellers produce mixing, while the disks do not.

2. The "base" flow

To dissect the mixing mechanism in this (or any other) flow, it is useful to separate the dominant, large-scale, circulatory flow from the small-scale flows affected by particular details, e.g. impeller design. The dominant flow is revealed in Fig. 1(b), where we show dye advection snapshots taken from experiments using co-axial disks, which for our purposes represent idealized, featureless impellers. Although isolated disks, in either symmetric or asymmetric (Fountain, Khakhar, & Ottino, 1998) arrangements, are not found in industrial practice, this simplified flow can be used to understand more realistic systems. In the top half of Fig. 1(b), we show a photograph of multiple dye streaks from an experiment in which dye was injected at several different locations into a flow produced by steadily rotating the disks at 100 rpm ($\mathrm{Re} = \rho N D^2/\mu \approx 40$, where ρ is density, N is revolutions per second, D is diameter, and μ is viscosity). Red fluorescent dye was injected near the center of the tank, producing the red torus after 30 min of mixing; green dye subsequently injected above that has been mixed for 15 min, illuminating a second torus. Dye was then injected into the uppermost green region, which has been mixed for 7 min, and finally into the red region surrounding this, which has been mixed for 2 min. Each of these regions remain separate during their respective blending times. The tori also do not mix with one other: the lowest, red, dye stream in the top half of Fig. 1(b) was injected 30 min before the photograph was taken and has begun to diffuse, but remains within a toroidal envelope and displays no detectable mixing with the green dye stream immediately above.

[1] The kinetic energy of the impeller system is 70.4 J, as compared with 68.8 J for the disk system. Kinetic energies are determined by summing over tetrahedra tesselating the container in a direct computational fluid dynamic simulation of the flow.

The fact that mixing does not occur either within or between the toroidal envelopes in the tank stirred by disks can also be seen in a slice through the tank axis, shown in the bottom half of Fig. 1(b). In this photograph, fluorescent dye has been distributed throughout the tank, and the disks have been rotated for 10 min at 100 rpm. The tank was then illuminated with a laser sheet, revealing closely spaced, concentric sets of rings, which demonstrate that fluid does not mix down to very small length scales. In addition, the sets of nested tori are separated from one another by separatrices that begin and end either in hyperbolic or parabolic rings. This is as we would expect, since the flow is steady and (since every azimuthal slice through the mixer is identical) effectively two-dimensional. In such a system, it has been known for over a century (Strogatz, 1994) that fluid must follow closed, nonmixing, trajectories, and mixing can only occur slowly, by virtue of diffusion.

3. The mechanism of chaotic mixing in stirred tanks

Evidently, stirring action alone does not generate detectable global mixing. How then does mixing occur in practical systems? To address this question, we analyze perturbations of the dominant circulatory flow, introduced in our system by the passing of impeller vanes. Our point of departure is the observation, commented on earlier, that there is marked similarity between the flow structures and the energies dissipated in tanks stirred by disks and by impellers (Fig. 1(c)), from which we deduce that these perturbations must be small.

To illustrate this point, recall Fig. 1(a), a photograph of the tank stirred by multi-bladed impellers. In this experiment, two fluorescent dye injections were performed. Fifteen minutes before the photograph on the left of the figure was taken, dye was injected in the center of the tank. Fifty minutes after the first injection, a second aliquot of dye was injected into the same location, and after 15 min a second snapshot was taken, as displayed on the right of Fig. 1(a). The tank was run continuously at 100 rpm throughout the experiment. This double-injection technique exposes the isolated islands, which appear as six black spots in the photograph, alongside bright streaks of fluid revealing the short time dynamics of the mixing process.

Crucially, within the blue rectangle, magnified in Fig. 2(b), we see that the impellers produce fine, vertically oriented, ripples of dye. These ripples are absent from the disk system and reveal the mechanism for convective mixing. As they travel around the underlying convective loops, the ripples become compressed radially and elongated vertically, reoriented, and reinjected into new folds. During each pass through the impeller blades, the advected dye is repeatedly stretched and folded within an invariant template of vertical ripples, producing self-similar patterns of dye striations (Alvarez, Muzzio, Cerbelli, Adrover, & Giona, 1998). We can examine this mechanism in greater detail through

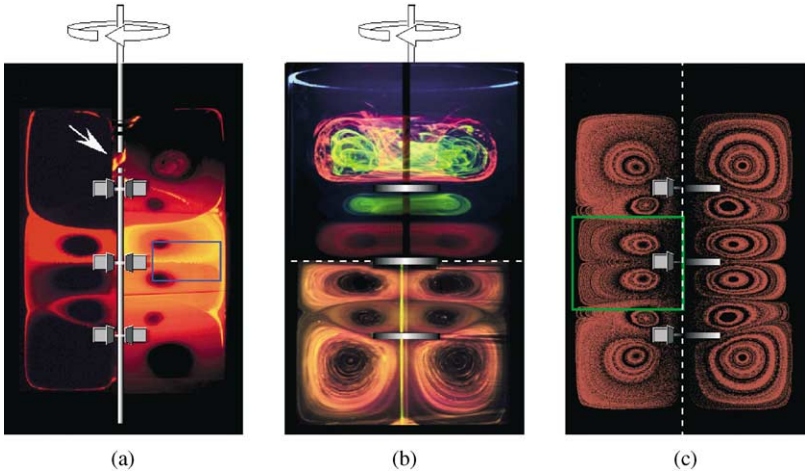

Fig. 1. Comparison between dye advection in a tank stirred by impellers, which mix, and by disks, which do not. (a) Mixing by three impellers in a cylindrical tank illuminated from the side by a laser sheet. In this double-injection experiment (see text), newly injected dye is yellow and previously dispersed dye is orange or red, depending on concentration. (b) Fully compartmentalized flow in the same tank stirred by three disks. In the top half of the figure, multiple dye injections reveal that there is no mixing either between or within nested tori (see text). The bottom half of the figure shows an experimental surface of section (see text). (c) Surface of section from numerical simulations of impellers (left) and disks (right) in tank identical to experiments. In all figures, the tank is 20 cm in diameter, the impellers have six flat, symmetrically placed vanes and are 6.6 cm maximum diameter, and the tank is filled to a height of 40 cm with glycerin. To compensate for optical distortion due to tank curvature, the tank is enclosed in a cubic chamber filled with refractive-index matched fluid.

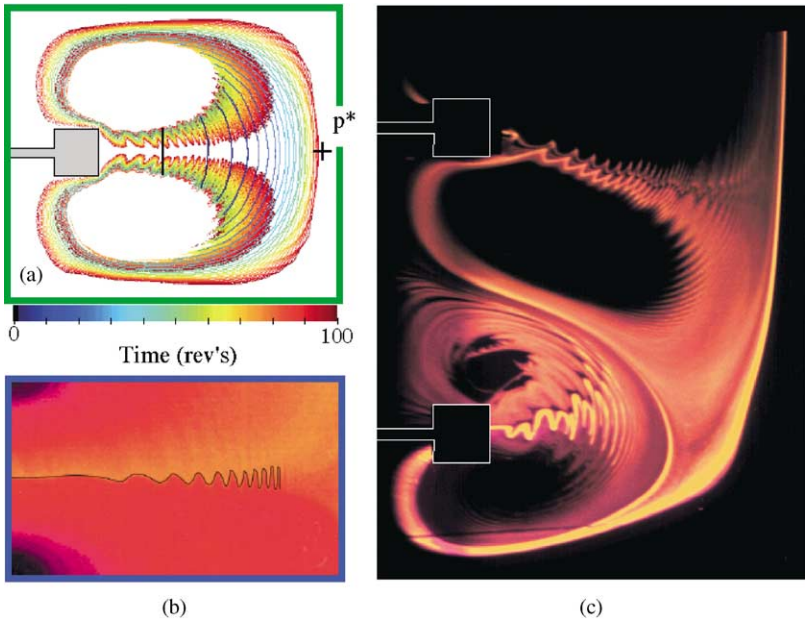

Fig. 2. Oscillatory structure in a three-Rushton impeller stirred tank. (a) Evolution of an initially vertical line of marker particles through 100 impeller revolutions on the surface of section shown inside the green box of Fig. 1(c). (b) Magnified view of the blue box from Fig. 1(a), showing ripples that are compressed radially and elongated vertically as they progress outward toward the fixed point, p^*. Location of maximum color gradient identified as black curve. (c) Dye injection experiment showing tracer trajectories generated by a three-Rushton impeller tank system in which the third, fifth and sixth vanes of the center impeller have been removed. The photograph displays only the middle and top impellers. The chain of waves emanating from the lower impeller exhibits an irregular structure because the vanes remaining in the impeller are not equally spaced.

numerical simulations (Zalc, Szalai, Alvarez, & Muzzio, 2002). In Fig. 2(a), we display a surface of section in which 30,000 marker particles, initially placed on the black vertical line to the right of the impeller vane, are computationally advected through 100 impeller revolutions. The geometry, fluid viscosity and impeller speed are identical to experimental conditions. The location of this region is indicated by the green box in the larger surface of section, Fig. 1(c).

The computations presented in this work were performed using the ORCA® CFD package (Dantec Dynamics; Mahwah, NJ) with a computational mesh of 370,340 nodes and 1,944,799 tetrahedra. The CFD solver used to obtain the velocity and pressure field was acuSolve (ACUSIM Software, Saratoga, CA), which solves the fully-coupled mass and momentum equations based on Galerkin/least-squares finite element method with equal-order interpolation for all field variables. The residuals for both velocity and pressure were required to converge below 10^{-4} dimensionless units. Additional details of the solver technology and post-processing routines, as well as detailed information about accuracy and convergence of the cases presented in this paper, are provided elsewhere (Zalc, Alvarez, & Muzzio, 2001). For the computations performed here, no-slip boundary conditions were specified at the solid walls of the vessel and zero stress at the top surface, which is the same as in the experiments.

Three things are notable from the computational results. First, from Fig. 2(a), we see that a line of initially vertical markers remains smooth and unfolded as it is advected past the parabolic fixed point, p^*. Second, folding is introduced exclusively during passage of the markers past the impeller vanes. In Fig. 2(a), we color code intersections based on the time at which they pierce the fixed plane (see legend beneath the figure). Evidently, the convected line remains entirely smooth throughout its circuit until it passes near the impeller vanes, which first occurs after about 30 impeller revolutions. At this point, well-defined and reproducible folds emerge, each of which defines a chaotic "horseshoe" (Strogatz, 2001). It is well known (Wiggins, 2001) that one folding operation in a periodic flow implies infinitely many, causing volume elements to stretch characteristically exponentially in time. We emphasize that although the Lagrangian mixing pattern becomes quite complex through the repeated application of horseshoe dynamics, the Reynolds number is under 100 and the Eulerian flow remains laminar. Although these horseshoe folds are not evident in a long time surface of section (Fig. 1(c)) because the dye homogenizes and displays a structureless pattern, they are manifest in the transient portrait of Fig. 2(a). Thus we find that in the stirred tank, stretching and folding are almost entirely decoupled: smooth stretching occurs (in both the disk and impeller configurations) as fluid approaches parabolic and hyperbolic points such as p^*, while folding occurs as a result of passage of fluid around the impeller vanes.

Third, while large regions of the flow are chaotic, the exchange of material between compartments of the tank is slow and occurs through a complex route. From Fig. 1(a), it is evident that fluid in the third compartment from the top travels upward along a narrow channel beside the tank wall, bypassing the second compartment, to encircle the topmost compartment and form a thin ribbon around the shaft (arrow in Fig. 1(a)), finally entering the top compartment from beneath. Thus, longer range transport occurs between *alternating* sequences of cells, and neighboring cells often only communicate indirectly. Consequently, introducing more turbine elements—a standard industrial procedure—is of questionable utility.

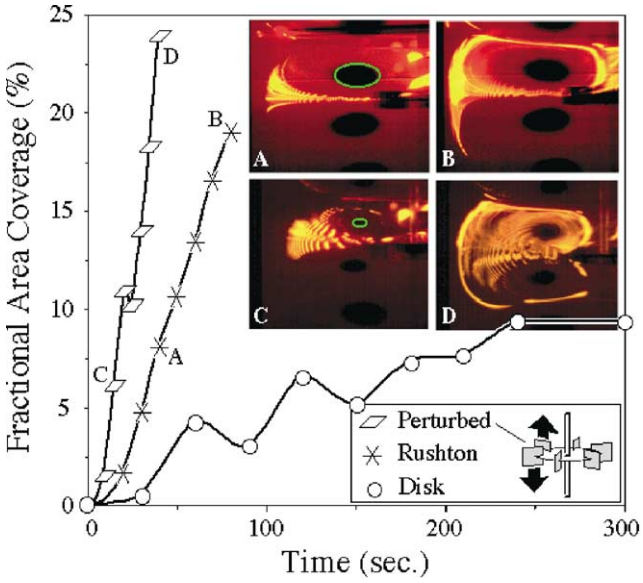

Fig. 3. Experimental stretching of dye for disk, Rushton, and perturbed-Rushton impeller designs. In each case, three impellers at the same locations are used, and the amount and location of dye injection were made as similar as experimentally feasible. The Rushton and perturbed-Rushton exhibit rapid stretching of dye through the repeated action of horseshoe dynamics, while the disk impeller displays much slower stretching. The oscillations in the disk case occur as the centroid of the dye blob travels around the tank. The labelled insets are photographs showing typical stretching behavior in identical regions of the tank (surrounding the blue rectangle shown in Fig. 1(a)). The labels correspond to data points shown in the main plot. We digitize these photographs, taken at regular time intervals, and threshold the image to compute the fractional area containing dye.

To confirm experimentally that the ripples observed are caused by flow perturbations introduced by the impeller vanes, three of the six vanes from the central impeller are removed, and a dye injection experiment is then performed. Fig. 2(c) shows the upper right quadrant of the mixing tank illuminated by a laser sheet for this new system. Well ordered periodic ripples emanating from the central impeller are now replaced with repeated "m"-shaped ripples, as first a single vane, and then two vanes in sequence, pass through the fluid. In both standard and perturbed impeller configurations, an invariant template of self-similar mixing striations is apparent, however, the change in impeller design has manifestly produced a distinct template near the lower impeller. Comparing Fig. 2(b) with (c), the ripples are significantly larger for the impeller with missing vanes than for the standard impeller. Apparently, the impeller with missing vanes introduces larger perturbations than the standard one, which perturbs the flow more often, but to a lesser extent each time.

We quantify the mixing behavior by digitally processing multiple images taken at regular intervals from dye injection experiments. Sample images are shown in the insets to Fig. 3(a), as described in the figure caption. We threshold each image to remove the background, and evaluate the number

of illuminated pixels as a function of time. This number, normalized to the imaged area, is shown in the main plot of Fig. 3 for three separate experiments. In the first experiment, the three disks of Fig. 1(b) result in the slowest, nearly linear, growth of area coverage, indicated by open circles in Fig. 3. In the second experiment, the standard three-impeller design introduced in Fig. 1(a) is studied. This leads to much more rapid dye dispersion, displayed as asterisks in Fig. 3. In the third experiment, the fact that the mixing dynamics depends sensitively on flow past the impeller is used to improve the mixing rate by making a small modification to the impeller design. Specifically, one of the vanes in the central impeller is moved upward by half the vane height, and one adjacent vane is moved downward by the same distance, as sketched in the legend to Fig. 3. In this case, represented by oblique symbol, the growth is more rapid still, achieving the area coverage attained using the standard design in half the time. Also evident from the inset photographs, the size of the non-chaotic islands is significantly reduced: the black islands circled in green in insets A and C are decreased in area by more than a factor of 10. Other design modifications including changing impeller blade size and frequency are also under active investigation in our laboratory.

4. Conclusions

Our experiments and simulations demonstrate that flow in one of the most common practical mixers is almost identical to a dominant non-chaotic circulatory flow. Mixing occurs only due to small perturbations to a non-chaotic flow that lead to the emergence of 3D horseshoes. Evidently, the laminar ST operates very close to integrability, which explains why these systems are so inefficient, requiring many thousands of flow iterations to achieve their asymptotic (often incomplete) degree of homogeneity—because of the small size of the perturbations that are responsible for mixing, most of the power expended in mechanical stirring produces no detectable mixing at all. We believe that the stirred tank represents a fruitful archetype for the application of dynamical systems tools that, to date, remain to be exploited in mixing problems of everyday interest.

References

Alligood, K. T., Sauer, T. D., & Yorke, J. A. (1996). *Chaos*: *An introduction to dynamical systems* (p. 49). New York: Springer.

Alvarez, M. M., Muzzio, F. J., Cerbelli, S., Adrover, A., & Giona, M. (1998). *Physics Review Letters*, *81*, 3395–3398.

Aref, H. (1984). *Journal of Fluid Mechanics*, *143*, 1.

Epstein, I. R. (1995). *Nature*, *374*, 321.

Fountain, G. O., Khakhar, D. V., & Ottino, J. M. (1998). *Science*, *281*, 683.

Graham, M. D., Kevrekidis, I. G., Asakura, K., Lauterbach, J., Krischer, K., Rotermund, H. -H., & Ertl, G. (1994). *Science*, *264*, 80K.

Graziosi, P. (1960). *Paleolithic art* (p. 120). New York: McGraw-Hill.

Harnby, N., Edwards, M. F., & Nienow, A. W. (1992). *Mixing in the process industries* (p. 10). New York: Butterworth-Heinemann.

Harvey, A. D., & Rogers, S. E. (1996). *AIChE Journal*, *42*, 2701.

Harvey, A. D., Wood, S. P., & Leng, D. E. (1997). *Chemical Engineering Science*, *52*, 1479.

Kalk, J., & Langlykke, A. (1986). *ASM manual of industrial microbiology and biotechnology*.

Lamberto, D. J., Alvarez, M. M., & Muzzio, F. J. (2001). *Chemical Engineering Science*, *56*, 4887.

Majda, A. J., & McLaughlin, R. M. (1993). The effect of mean flows on enhanced diffusivity in transport by incompressible periodic velocity fields. *Studies on Applied Mathematics*, *89*, 245–279.

Nuclear safety, (1995). *Concerns with nuclear facilities and other sources of radiation in the former Soviet Union*. Letter report, 11/07/95, GAO/RCED-96-4.

Pierrehumbert, R. T. (1991). *Geophysical and Astrophysical Fluid Dynamics*, *58*, 285–319.

Ranade, V. V. (1997). *Chemical Engineering Science*, *52*, 4473.

Sommerer, J. C., & Ott, E. (1993). *Science*, *259*, 335.

Strogatz, S. H. (1994). *Nonlinear dynamics and chaos* (p. 203). Reading, MA: Addison-Wesley.

Strogatz, (2001). Extensive validation of computed laminar flow fields in a stirred tank equipped with three Rushton turbines. *AIChE Journal*, *47*(10), 425.

Tanguy, P. A., Thibault, F., Brito-de la Fuente, E., Espinosa-Solares, T., & Tecante, A. (1998). *Chemical Engineering Science*, *52*, 1733.

de la Villéon, J., Bertrand, F., Tanguy, P. A., Labrie, R., Bousquet, J., & Lebouvier, D. (1998). *AIChE Journal*, *44*, 972.

Wiggins, (2001). Extensive validation of computed laminar flow fields in a stirred tank equipped with three Rushton turbines. *AIChE Journal*, *47*(10), 425.

Zalc, J. M., Alvarez, M. M., & Muzzio, F. J. (2001). Extensive validation of computed laminar flow fields in a stirred tank equipped with three Rushton turbines. *AIChE Journal*, *47*(10), 2144.

Zalc, J. M., Szalai, E. S., Alvarez, M. M., & Muzzio, F. J. (2002) *AIChE Journal*, accepted for publication.